FDTD modeling of phase grating diffusion

Konrad Kowalczyk
Multimedia Communication and Signal Processing (LMS)
University of Erlangen-Nuremberg
91058 Erlangen, Germany
Email: kowalczyk@lnt.de

Maarten van Walstijn
Sonic Arts Research Centre (SARC)
Queen's University of Belfast
BT7 1NN Belfast, United Kingdom
Email: m.vanwalstijn@qub.ac.uk

***Abstract*—In this paper, a method for modeling diffusion caused by non-smooth boundary surfaces in simulations of room acoustics using finite-difference time-domain (FDTD) technique is investigated. This approach adopts the well-known theory of phase grating diffusers to efficiently model sound scattering from rough surfaces. The variation of diffuser well-depths is attained by nesting allpass filters within the reflection filters from which the digital impedance filters used in the boundary implementation are obtained. The presented technique is appropriate for modeling diffusion at high frequencies caused by small surface roughness and generally diffusers that have narrow wells and infinitely thin separators. Good agreement with acoustic theory is confirmed by numerical measurements of the diffusion coefficient for various types of non-smooth boundaries.**

***Index Terms*—Acoustic signal processing, acoustic scattering, acoustic refraction, architectural acoustics, digital filters, fractals**

I. Introduction

Sound diffusion in rooms is a perceptually important acoustic phenomenon that includes scattering of reflected sound waves from not perfectly smooth surfaces and edge diffraction effects. Since the wave-based methods inherently model all natural wave-related phenomena such as edge diffraction, they can in general be used to predict the performance of diffusers. The finite-difference time-domain (FDTD) method has recently emerged as a suitable wave-based technique for investigation of surface diffusion [1], [2], where an irregular boundary shape was represented directly in the grid topology. Quadratic residue diffusers modeled with integer length delay lines incorporated in 1-D reflection filters were also investigated using a mathematically equivalent digital waveguide mesh (DWM) technique, e.g. in [3]. However, commercially available diffusers aim to create strong scattering at a given design frequency and they do not allow for a full control over the diffusive properties of a wall, which is particularly important for auralization applications. A method for controllable diffusion using circulant matrices that result in random redirection of reflected waves at the mesh nodes adjacent to the boundary was investigated in [4]. However, this so-called "diffusing layer" is unphysically placed in front of the boundary and the point-based scattering mechanism makes this model unpredictable for waves arriving at high angles of incidences [4].

The approach taken in this paper enables a convenient yet physical modeling of surface diffusion in FDTD room acoustic simulations by varying the acoustic impedance along the boundary surface. This approach is based on spatial variation of the 'local well depth' typical for phase-grating diffusers [5], and it is additionally suitable for modeling controllable diffusion from rough surface shapes with fractional Brownian diffusers [6].

II. Modeling phase grating diffusion

A. Motivation

Considering a locally reacting boundary (which is a typical assumption in the context of room acoustic modeling), the absorbing properties of the wall are mainly dependent on the material from which the boundary is constructed, and hence they should be defined locally. On the other hand, surface diffusion is caused by irregularities along the boundary in either shape or impedance, and thus they cannot be defined for a single boundary point. Therefore, in this paper we formulate the physical boundary model that maintains (as much as possible) the separation between these two acoustic phenomena by defining the boundary absorbtion locally and creating surface diffusion by varying spatially the reflection phase.

B. Phase Grating using Boundary Filters

Frequency-dependent absorption and diffusion are simultaneously captured by representing each boundary node by an impedance filter designed from a normal-incidence reflection filter $R_0(z)$, which consists of an absorption filter in cascade with a fractional delay filter,

$$R_0(z) = R_a(z)\, R_d(z), \tag{1}$$

where $R_a(z)$ is a digital reflection filter designed to match the absorptive properties of the boundary material (see [7] for the design strategy) and R_d is a fractional delay filter that represents a local 'well-depth'. Surface diffusion is realized by spatial varying the delay lengths across the boundary surface, which model spatial variation of the 'local well depth'. In general, such delays can be of non-integer length, and thus the so-called fractional delay filters with maximally flat amplitude response should be used to enable full control over local (point-wide) absorption through absorption filter $R_a(z)$ only. For this purpose, Thiran allpass filters [8] are suitable approximations due to their strictly allpass magnitude characteristic and a flat phase delay response at low frequencies.

Furthermore, this is the only design technique that provides the closed-form solution for designing allpass interpolators of arbitrary order [9]. Since the stability and accuracy of the Thiran allpass filter approximating the fractional delay of D samples requires the use of roughly the same value of the filter order M (i.e., $[M - 0.5 \leq D < M + 0.5$), it is proposed to employ the first- or second-order Thiran allpass filter in cascade with a delay line for efficient modeling of long fractional delays [9], as depicted in Fig. 1. The transfer function of the delay filter $R_d(z)$ then reads

$$R_d(z) = A(z) \;\; z^{-N}, \tag{2}$$

where $A(z)$ denotes the M-order Thiran allpass filter and z^{-N} denotes a delay line of $N = D - M$ delays. Finally, the normal-incidence reflection filter $R_0(z)$ can be converted into the digital impedance filter $\xi_w(z)$ that represents the local specific acoustic impedance according to

$$\xi_w(z) = \frac{1 + R_0(z)}{1 - R_0(z)}, \tag{3}$$

and implemented using the digital impedance filter (DIF) boundary model proposed in [7].

C. DIF boundary model

Since the results from numerical experiments presented in this paper were generated using the 2-D standard leapfrog scheme, the appropriate update formula for the boundary node is given by [7]

$$p_{l,m}^{n+1} = \Big[\lambda^2(2p_{l-1,m}^n + p_{l,m+1}^n + p_{l,m-1}^n) + 2(1 - 2\lambda^2)p_{l,m}^n + (\frac{\lambda a_0}{b_0} - 1)p_{l,m}^{n-1} + \frac{\lambda^2}{b_0}\, g^n\Big] \;/\; \Big(1 + \frac{\lambda a_0}{b_0}\Big), \tag{4}$$

where the filter input x and output y values are defined as

$$x^n = \frac{a_0}{\lambda b_0}(p_{l,m}^{n+1} - p_{l,m}^{n-1}) - \frac{g^n}{b_0}, \tag{5}$$

$$y^n = \frac{1}{a_0}\Big(b_0\, x^n + g^n\Big), \tag{6}$$

and the intermediate value g is given by

$$g^n = \sum_{i=1}^{N} \Big(b_i\, x^{n-i} - a_i\, y^{n-i}\Big), \tag{7}$$

where $p_{l,m}^n$ is the pressure variable at grid point l, m at time $t = nT$, and $a_0, a_1, ..., a_N$ and $b_0, b_1, ..., b_N$ are the impedance filter nominator and denominator coefficients, respectively. $\lambda \leq 1/\sqrt{2}$ denotes the Courant number which is typically set at its top value for the highest accuracy.

D. Well depth and delay length

In order to model diffusers with the desired well depth d, the corresponding value of the fractional delay D (that is modeled by delay filter $R_d(z)$) should be set according to

$$D = \frac{d}{cT}, \tag{8}$$

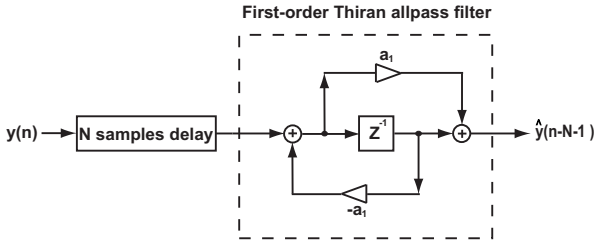

Fig. 1. A diagram depicting a delay line in series with a first-order Thiran allpass filter.

where c is the sound wave velocity and $T = 1/f_s$ is the time step. Thus it can be seen that the effective well depth depends on the simulation's sampling frequency. It should also be mentioned that due to the dispersion error (i.e., a numerical artefact of wave-based methods), the wave propagation speed in FDTD simulations can differ from c depending on the propagation direction. However, since the delay length cannot be adjusted simultaneously for all directions, (8) constitutes the best overall design choice.

E. Controlling diffusion

In this section, the method for controlling the amount of diffusion based on fractional Brownian diffusers [6] is described. To design a Brownian diffuser, we first generate the white noise sequence of length equal to the number of boundary grid points. Such a sequence is next spectrally shaped with the use of a digital filter designed to match values of the diffusion coefficient in each frequency band. Simple spectral shaping is possible with a linear roll off filter, which has the gain given by

$$G(f) = \frac{1}{f^{\beta/2}}, \tag{9}$$

where β denotes the spectral density exponent that should be set within the range of 1 and 3 to preserve the 1-D fractal shape. The amount of diffusion is controlled by setting parameter β. For high values of β, the surface is smooth in shape and the resulting diffusion is less pronounced. On the other hand, for small values of β, the surface shape is very spiky, and as a consequence strong diffusion is created.

The lowest frequency f_0 at which diffusion effectively occurs depends on the maximum well depth d_m,

$$f_0 = \frac{c}{2d_m}, \tag{10}$$

and it is analogous to the design frequency of quadratic residue diffusers [10]. However, in practice diffusion actually begins from around an octave below this theoretical frequency to create strong diffusion already at f_0.

III. Results of numerical experiments

The setup for numerical experiments follows the guidelines for measuring the diffusion coefficient defined in the AES standard [11]. A perfectly reflective diffuser sample of width 1.1m was placed in the middle of a large room of size 44m

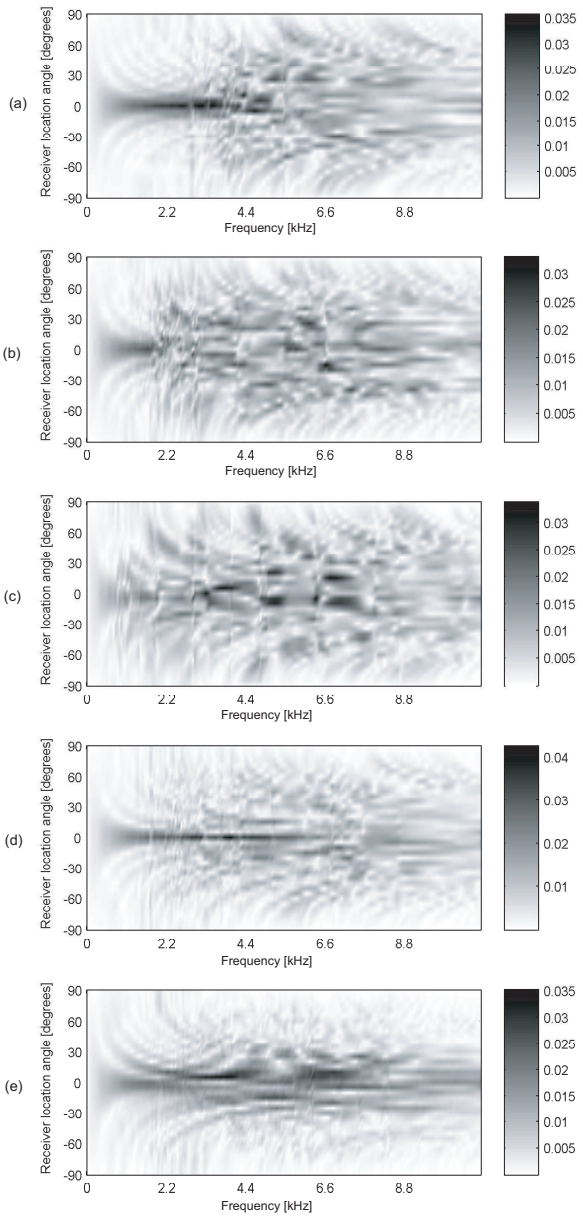

Fig. 2. The pressure magnitude of the reflected signal for all receiver positions located on a semicircle for the following boundary surface shape: (a) a white noise with $D_{max} = 5$ samples, (b) white noise with $D_{max} = 10$ samples, (c) white noise with $D_{max} = 20$ samples, (d) Brownian noise with $\beta = 1.73$ and $D_{max} = 10$ samples, (e) Brownian noise with $\beta = 3$ and $D_{max} = 10$ samples.

x44m (in order to avoid wall reflections) modeled using the 2-D standard leapfrog scheme at the sample rate of 44.1 kHz. In successive measurements, the source position was changed with an angular separation of 10^o on a semicircle with a radius of 7.7 m, whereas a set of omnidirectional receivers was placed on a semicircle with a radius of 4.4m. The measured impulse responses were transformed to the frequency domain, the sound pressure level in each one-third octave band was computed, and finally the random-incidence diffusion coefficient (as defined in [11]) for each diffuser was

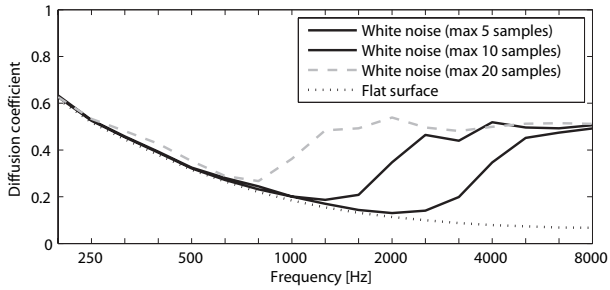

Fig. 3. Random-incidence diffusion coefficient for a white-noise like boundary shape with the maximum roughness expressed in terms of the number of delay samples $D_{max} = 5, 10, 20$ samples.

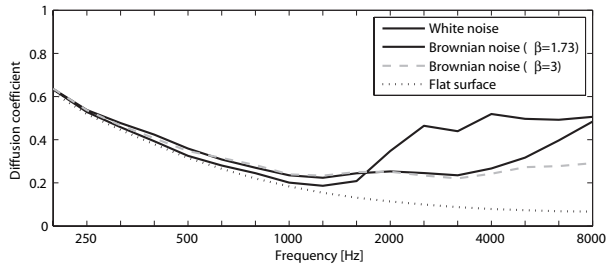

Fig. 4. Random-incidence diffusion coefficient for a white-noise (black solid line), Brownian noise with $\beta = 1.73$ (gray solid line), and Brownian noise with $\beta = 3$ (black dashed line); the maximum roughness of 10 delay samples.

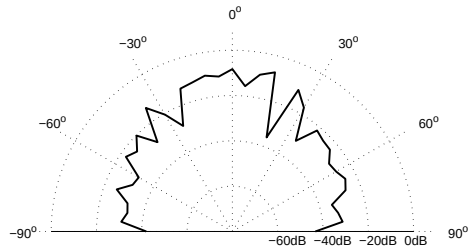

Fig. 5. Polar magnitude plot for the Brownian noise-like boundary sample with the maximum depth corresponding to 10 delays and $\beta = 3$, at frequency $f = 5$kHz.

calculated. Three sequences of length 101 were generated to investigate the performance of the fractional Brownian diffuser sample: the white noise sequence and two Brownian noise sequences that resulted from spectral shaping of the Gaussian noise with spectral density exponent values respectively set as $\beta = 1.73$ and $\beta = 3$.

A. Spatial diffusion and diffusion coefficient

The pressure magnitude results for a set of white noise sequences with the maximum delay values (corresponding to the maximum depth of the diffuser) of $D = (5, 10, 20)$ samples, and two Brownian noise sequences shaped with $\beta = 1.73$ and $\beta = 3$ at the maximum delay value of $D = 10$ are illustrated in Fig. 2. These three delay values correspond to the following design frequencies $f_0 = 4.410$ kHz,2.205 kHz, 1.102 kHz, respectively, as can be calculated from (8) and (10). Fig. 2(b-d) indicates that the specular reflection is very well spatially scattered by a white-noise shaped boundary for

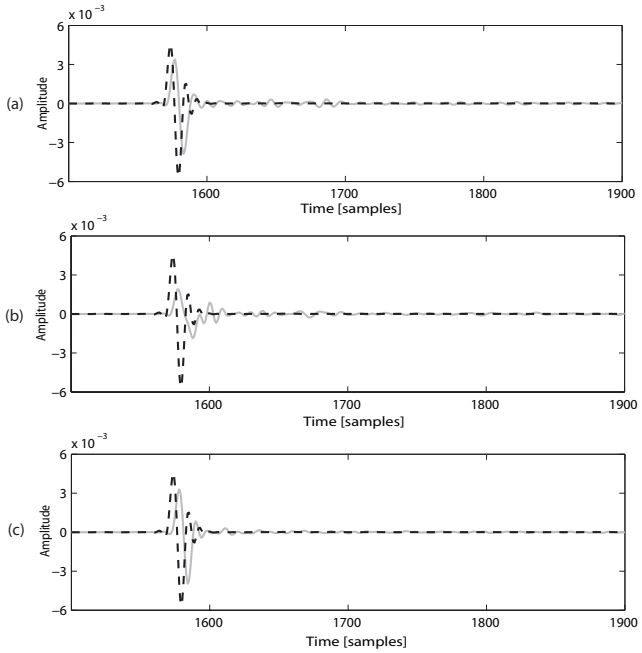

Fig. 6. The signal reflected from the sample diffuser (gray solid line) plotted against the signal reflected from the flat boundary sample (black dashed line) in the time domain for the following diffusers: (a) a white-noise boundary surface shape with the maximum depth corresponding to 5 delays, (b) a white-noise boundary surface shape with the maximum depth corresponding to 10 delays, and (c) a Brownian-noise like boundary surface shape with the maximum depth corresponding to 10 delays and $\beta = 3$.

frequencies above the respective design frequency, and some slight diffusion also occurs half an octave below the design frequency. Strong diffusivity of white-noise shaped diffusers is confirmed by high diffusion coefficient values above the design frequency, as depicted in Fig. 3. For comparison of Brownian diffusers, spatial scattering from the three noise-shaped boundaries (white-noise and two Brownian-noise sequences) for the design frequency of 2.205 kHz is illustrated in Fig. 2(c,e,f). In contrast to even scattering in many directions that results for the white-noise shape, the Brownian shape yields scattering in a reduced number of reflection directions. Increasing the value of the spectral density exponent, spatial scattering decreases, which can also be observed in diffusion coefficient plots illustrated in Fig. 4. The low diffusion coefficient value for $\beta = 3$ can be explained by investigating spatial scattering in Fig. 2(f), where the incident sound wave is redirected in a few directions rather than scattered in multiple directions, which is also exemplarily shown in a polar magnitude plot for a frequency $f = 5$kHz in Fig. 5.

B. Time spreading

In addition to spatial scattering, time spreading of the reflected sound wave plays a significant role in the overall diffusion effect, the influence of which is particularly important for phase grating diffusers. Since such a time spreading aspect of sound scattering is not effectively captured by the diffusion coefficient, time-domain analysis of the reflected sound wave from the diffuser sample is presented in this section. The comparison of two white-noise boundary shapes for the design frequency of $f_0 = 4.410$ kHz and $f_0 = 2.205$ kHz, and a Brownian diffuser with $\beta = 3$ and $f_0 = 2.205$ kHz are illustrated in Fig. 6; a signal reflected for a highly reflective flat sample is also included as a reference. Comparing Fig. 6(a) and (b), it can be seen that time spreading is stronger for the diffuser characterized by a larger maximum depth. Comparing the boundary shapes of diffusers based on white and Brownian sequences for the same design frequency $f_o = 2.205$kHz in Fig. 6(b) and (c), a more spiky surface shape clearly increases the time spreading properties.

IV. Conclusions

In this paper, a method for modeling surface diffusion from rough boundaries in FDTD simulations of room acoustics is presented. Surface diffusion is modeled by shaping the surface geometry through spatial varying the boundary impedance filters, whereas absorption is specified locally for each boundary node. Spectral shaping of Gaussian noise have been shown to offer a good control over the amount of diffusion by defining the maximum depth and the variation smoothness of the boundary surface shape. Spatial scattering and time spreading results confirm the validity of this approach.

V. Acknowledgements

The authors would like to thank Dr Damian T. Murphy of the University of York for insightful comments on the presented topic.

References

[1] T. Yokota, S. Sakamoto, and H. Tachibana, "Visualization of sound propagation and scattering in rooms," *Acoust. Sci & Tech.*, vol. 23, no. 1, pp. 40–46, 2002.

[2] J. Redondo, R. Picó, and B. Roig, "Time domain simulation of sound diffusers using finite-difference schemes," *Acta Acustica united with Acustica*, vol. 93, no. 12, pp. 611–622, 2007.

[3] K. Lee and J.O. Smith, "Implementation of a highly diffusing 2-d digital waveguide mesh with a quadratic residue diffuser," *Proc. Int. Comp. Music Conf. (ICMC)*, pp. 309–315, November 2004, Miami, Florida.

[4] S. Shelley and D.T. Murphy, "The modeling of diffuse boundaries in the 2-D digital waveguide mesh," *IEEE Trans. on Audio, Speech and Language Processing*, vol. 16, no. 3, pp. 651–665, March 2008.

[5] M.R. Schroeder, "Binaural dissimilarity and optimum ceilings for concert halls: More lateral sound diffusion," *J. Acoust. Soc. Am.*, vol. 65, no. 4, pp. 958–963, 1979.

[6] T.J. Cox and P. D'Antonio, "Fractal sound diffusers," *103rd Convention Audio Eng. Soc.*, September 1997, Preprint 4578, New York, NY.

[7] K. Kowalczyk and M. van Walstijn, "Modeling frequency-dependent boundaries as digital impedance filters in FDTD and K-DWM room acoustics simulations," *J. Audio Eng. Soc.*, vol. 56, no. 7/8, pp. 569–583, 2008.

[8] T.I. Laakso, V. Välimäki, M. Karjalainen, and U.K. Laine, "Splitting the unit delay - tools for fractional delay filter design," *IEEE Signal Processing Magazine*, vol. 13, no. 1, pp. 30–60, January 1996.

[9] J.O. Smith, *Physical Audio Signal Processing for Virtual Musical Instruments and Digital Audio Effects*, W3K Publishing, http://books.wk3.org, August 2006.

[10] M.R. Schroeder, "Diffuse sound reflcetion by maximum-length sequences," *J. Acoust. Soc. Am.*, vol. 57, no. 1, pp. 149–150, 1975.

[11] AES 4id 2001(r2007), "AES information document for room acoustics and sound reinforcement systems - characterisation and measurement of surface scattering uniformity," *J. Audio Eng. Soc.*, vol. 49, pp. 149–165, November 2001.